REPORT DOCUMENTATION PAGE

Form Approved
OMB No. 0704-0188

1. REPORT DATE *(DD-MM-YYYY)*
09/28/2019

2. REPORT TYPE
Final Technical Report

3. DATES COVERED *(From - To)*
07/01/2018-06/30/2019

4. TITLE AND SUBTITLE
Dynamics, Impacts, and Predictability of Coupled Ocean-Atmosphere Interactions in the Northern Indian Ocean

5a. CONTRACT NUMBER

5b. GRANT NUMBER
N00014-15-1-2588

5c. PROGRAM ELEMENT NUMBER

6. AUTHOR(S)
Seo, Hyodae

5d. PROJECT NUMBER

5e. TASK NUMBER

5f. WORK UNIT NUMBER

7. PERFORMING ORGANIZATION NAME(S) AND ADDRESS(ES)
Woods Hole Oceanographic Institution
266 Woods Hole Road, MS 21
Woods Hole, MA 02543

8. PERFORMING ORGANIZATION REPORT NUMBER
WHOI-13258800

9. SPONSORING/MONITORING AGENCY NAME(S) AND ADDRESS(ES)
Dr. Scott Harper, Code 32
Physical Oceanography
Office of Naval Research
875 N. Randolph Street
Arlington, VA 22203-1995

10. SPONSOR/MONITOR'S ACRONYM(S)

11. SPONSOR/MONITOR'S REPORT NUMBER(S)

12. DISTRIBUTION/AVAILABILITY STATEMENT
Approved for public release; distribution is unlimited.

13. SUPPLEMENTARY NOTES

14. ABSTRACT
The project has two main threads that are aptly aligned with the ONR ASIRI and NASCAR DRIs. For the Bay of Bengal (BoB), we explore the sensitivity of the monsoon wind and rainfall variability to local air-sea coupling and remote influences based on various observational datasets and then use the regional models to quantify the impacts. For the Arabian Sea (AS), the regional coupled model was developed first, whereby the sensitivity of the air-sea coupling to the spatial scale of the oceanic variability is being examined.

15. SUBJECT TERMS
Ocean-atmosphere interactions

16. SECURITY CLASSIFICATION OF: a. REPORT	b. ABSTRACT	c. THIS PAGE	17. LIMITATION OF ABSTRACT	18. NUMBER OF PAGES	19a. NAME OF RESPONSIBLE PERSON
					Dr. Hyodae Seo
					19b. TELEPHONE NUMBER *(Include area code)*
U	U	U	UU	8	508-289-2792

Final Report: N00014-15-1-2588

Dynamics, Impacts, and Predictability of
Coupled Ocean-Atmosphere Interactions in the Northern Indian Ocean

Hyodae Seo
Physical Oceanography Department
Woods Hole Oceanographic Institution
Address: 266 Woods Hole Road, MS#21 Woods Hole, MA 02543
Email: hseo@whoi.edu

LONG-TERM GOALS

The overall objective of this project is to examine dynamics, impacts, and predictability of air-sea interaction in the Northern Indian Ocean, including the Bay of Bengal and the Arabian Sea. An orderly approach is proposed to achieve the following incremental goals: I) Elucidate the origin and dynamics of air-sea interactions through statistical, numerical and scaling analyses; II) Improve the simulation of the air-sea interactions by better representing the mixing, the barrier layer, and the diurnal cycle; III) Quantify the impacts of the air-sea interactions on the regional currents and the monsoon dynamics; and IV) Identify predictable components and predictability limits of the oceanic and atmospheric flows during and beyond the ONR observational programs.

OBJECTIVES

The objectives and immediate scientific goals of the proposed research are to

1) Develop a coupled ocean-atmosphere model that has significant and quantified skill in simulating the monsoon atmospheric circulation and its coupling with the ocean on intraseasonal time-scales (Long-term goals II & IV)
2) Examine sensitivities of the monsoon intraseasonal rainfall to upper ocean stratification, vertical mixing, barrier layer dynamics, and the diurnal cycle in the Bay of Bengal (Long-term goals I and II)
3) Explore the impact of thermal and mechanical air-sea coupling in the Arabian Sea on the regional ocean circulation (Long-term goal III) and their impact on the predictability of the monsoon rainfall over India (Long-term goal IV).

APPROACH

The project has two main threads that are aptly aligned with the ONR ASIRI and NASCAR DRIs. For the Bay of Bengal (BoB), we explore the sensitivity of the monsoon wind and rainfall variability to local air-sea coupling and remote influences based on various observational datasets and then use the regional models to quantify the impacts. For the Arabian Sea (AS), the regional coupled model was developed first, whereby the sensitivity of the air-sea coupling to the spatial scale of the oceanic variability is being examined.

TASKS COMPLETED

1) Quantified the distinct effects of thermal vs. mechanical air-sea coupling in the Arabian Sea.
2) Adopted a cross-spectral analysis approach to diagnosing of air-sea interaction across multiple scales in the Arabian Sea.
3) Examined the intraseasonal coupling between rainfall and SST in the Bay of Bengal and their interannual modulation by the Indian Ocean Dipole.
4) Explored the role of freshwater intrusions in the Bay of Bengal in the summertime upper ocean heat budget
5) Demonstrated the impacts of eddy-wind interactions on the energetics of the monsoon circulation and upper ocean stratification in the Bay of Bengal.

RESULTS

I. Arabian Sea Component

a. Distinct effect of air-sea interaction in the Arabian Sea (Seo 2017, JCLI).

We conducted a series of high-resolution SCOAR (WRF-ROMS) regional coupled model employing a novel coupling procedure to separate the spatial scale of the air-sea coupling through SST and surface current. The goal is to better understand the spatial scales at which the SST and ocean surface currents are coupled to the wind and evaluate their influences on coupled ocean-atmosphere circulation. Effect of mesoscale SST-wind interaction is manifested most strongly in wind work and Ekman pumping over the Great Whirl, primarily affecting its position and the separation latitude of Somali Current. If this effect is suppressed, enhanced wind work and weakened Ekman pumping dipole cause it to extend northeastward by 1° downstream. Current-wind interaction, in contrast, is related to the amount of wind energy input. When it is suppressed, especially due to background-scale currents, depth-integrated mean kinetic energy (MKE) and eddy kinetic energy (EKE) are significantly enhanced (as shown in Figure 1).

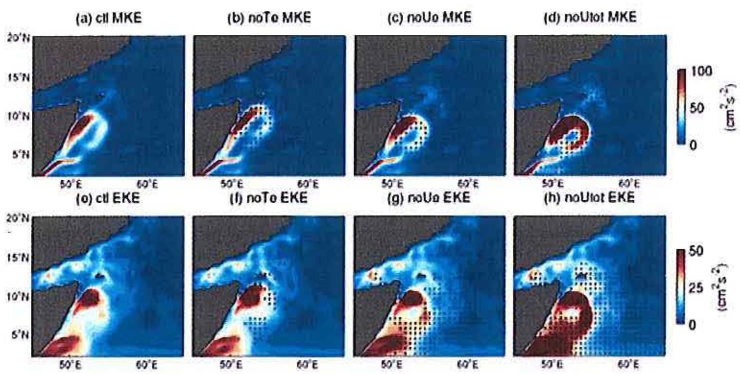

Figure 1: The 10-yr JJAS climatologies of MKE ($cm^2 s^2$) and EKE. Black dots denote the significant difference between each of the sensitivity simulations and CTL at the 95% confidence level.

Moreover, significant changes in time-mean SST and evaporation are generated in response to the current-wind interaction, accompanied by a noticeable southward shift in the Findlater Jet (Figure 2). The increase in moisture transport in the central AS implies that air-sea interaction mediated by the surface current is a potentially important process for simulation and prediction of the monsoon rainfall over India.

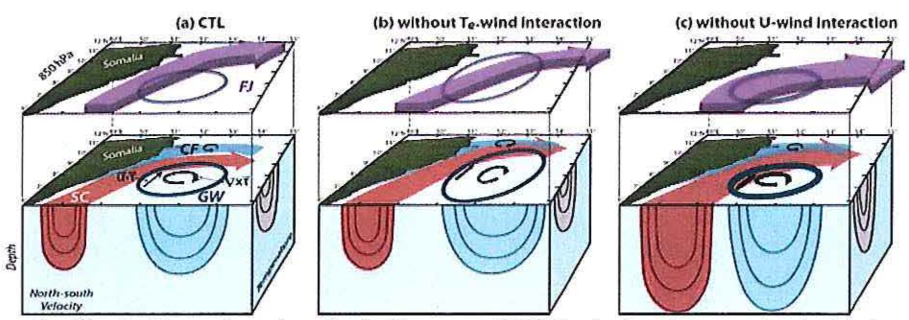

Figure 2: Schematic illustrations showing the influence of SST-wind and current-wind interactions: (a) The ocean panel of the CTL shows the summertime Somali Current (red arrow), Great Whirl (blue circle), cold filament (darker blue shading).

b. Scale-dependent diagnostics of air-sea interaction

The correlation or regression coefficient, commonly used as a diagnostic metric by the air-sea interaction community, does give an indication of the wind response to SST and surface current. However, it also includes contributions from broad scales that are represented in the high-pass filtered input fields, and so there is no useful information on the scale dependence in such calculations other than the gross separation of small scales from large scales. To quantify the coupling across multiple spatial scales, we have adopted a spectral-based approach, in which the transfer function, or gain factor, can be computed, which is equivalent to a regression coefficient that is computed as a function of wavenumber. The spectral transfer function and associated cross-spectral quantities (squared coherence and absolute phase) provide direct insights into the scale dependence of the relationship between two variables.

Figure 3 (left column) uses the ASCAT satellite wind stress and AMSR/AVHRR SST in the Arabian Sea to compute the squared coherence, gain factor, and phase factors as functions of the zonal wavenumber space and also latitude. The high squared coherence is found roughly in the 5-12°N latitude band and over wavelengths between 200 to 1000 km (the peak at 500 km). Gain factor varies in magnitude from 0.02 to 0.05 N/m^2 per °C over the 200-500 km wavelengths, where the absolute phase angle is < 90°, suggesting that at the 200-500 km wavelength scales in 5-12°N, SST and wind stress are positively correlated.

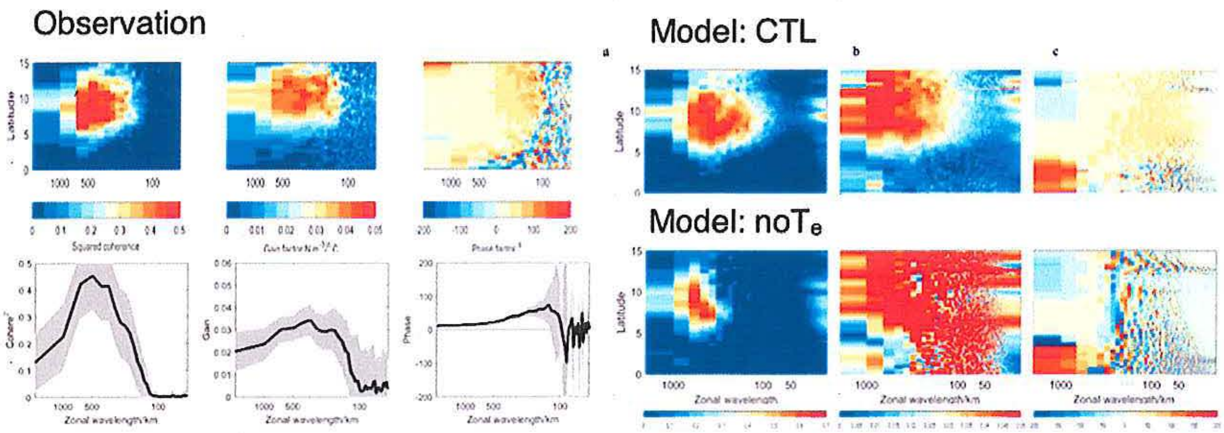

Figure 3: (Left Column) Squared coherence, gain, and phase factor of SST and wind stress in the Arabian Sea with the satellite data (2007-2011, Jun-Sep). (top) latitude-wavenumber diagram, (bottom) the average from 6 to 12°N. (Right Column) as in the observation but with CTL (top) and noTe (bottom).

Figure 3 (right column) shows the similar plots from the two model simulations, CTL and another run where the mesoscale SST effect on wind is suppressed (noTe). CTL can capture the salient feature of the observed SST and wind stress relationship in the wavenumber space, revealing the peak squared coherence at ~500 km wavelength over the 5-12°N. The gain factor is between 0.01-0.05 5N/m^2 per °C and the absolute angle less than 90°, indicating the positive correlation (SST impacting wind). When the SST in the coupled model is low-pass filtered to remove the wind response to mesoscale SST, the squared coherence is reduced. Though gain factor in noTe is much more enhanced than that of CTL and the satellite observations, the low squared coherence implies that this abnormal gain factor cannot be trusted.

II. Bay of Bengal Component

a. Intraseasonal air-sea interaction (Jongaramrungruang, Seo, and Ummenhofer et al. 2017)

We examined the physics of the observed ocean-atmosphere interactions on the intraseasonal (5-90 days) and interannual time-scales. Using satellite data and reanalysis products, we find that the intraseasonal ocean-atmosphere coupling remains significant during the Indian Summer Monsoon, with the maximum SST warming (cooling) preceding (following) the peak in the intraseasonal rainfall by 3-5 days (5-8 days) (Figure 4). The fact that the BoB SST leads the rainfall during the summer monsoons provides useful predictive information on the onset of the monsoon rainfall and its active/break cycles and points to the crucial need for real-time and sustained monitoring of the upper ocean processes in the BoB. Furthermore, the intraseasonal air-sea coupling exhibits striking interannual variability modulated by the Indian Ocean Dipole (IOD), the leading mode of interannual variability in the Indian Ocean. The intraseasonal SST variation and the rainfall are more pronounced in negative IOD years when the local BoB SST is anomalously higher. The atmospheric moisture budget analysis reveals that the enhanced intraseasonal coupling during the negative IOD years is primarily due to stronger moisture interchange between the ocean and atmosphere due to higher SST and moister atmosphere.

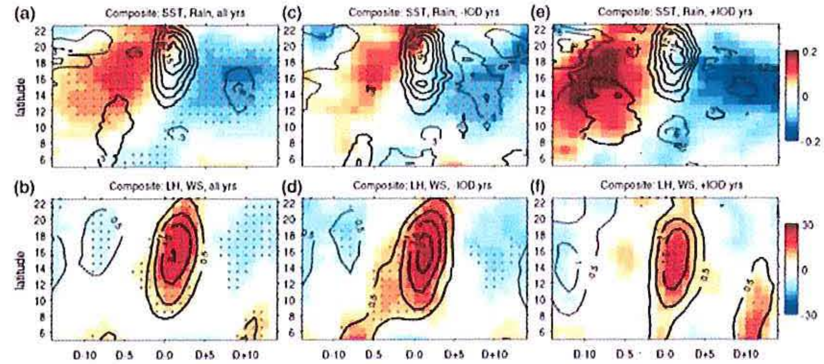

Figure 4: Lagged composite evolutions of the 5-90 day filtered (a) SST (color, °C) and rainfall (contours, mmday^{-1}) and (b) LH (shading, Wm^{-2}, positive out of the ocean) and wind speed (WS, ms^{-1}, contours) associated with the extreme intraseasonal rainfall events. Gray dots denote 90% significance level.

b. Impact of river plumes on the heat budget (Prend, Seo et al. 2018)

We further examined the moored observations at the ASIRI WHOI mooring at 18°N, 90°E in comparison to the RAMA moorings further south to understand the role of freshwater intrusion in the upper ocean temperature budget. Figure 5 shows the time-series of SST, SSS, and mixed layer depth (MLD) for the summer of 2015, color-coded to represent 4 moored locations along 90°E. At 18°N in late summer, the SSS shows the three distinctive river intrusion events. The arrival of river plumes results in extreme shoaling of the MLD. The low SSS signals and shoaled MLD can be seen as south as at 15°N with a delay of 15-20 days. In contrast, away from the river mouths at 12°N and 8°N, there is no sign of river intrusions. This striking north-south contrast of the MLD is reflected in the SSTs, showing enhanced 10-30 day SST variability in the northern two moorings. Moreover, the SST variability appears to be more energetic during late summer due to the river intrusions than during early summer.

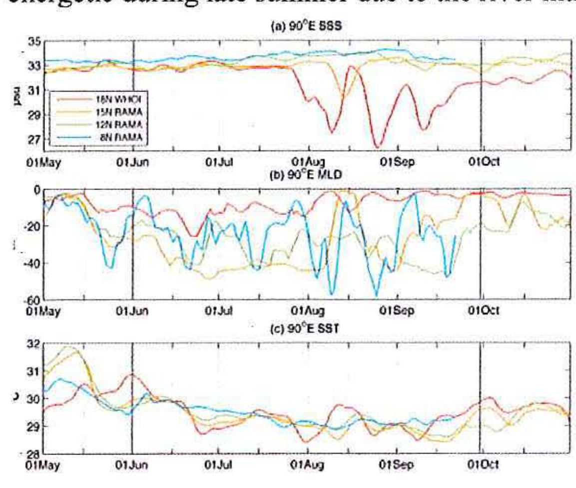

Figure 5: Observed daily (a) sea surface salinity (SSS, psu), (b) mixed layer depth (MLD, m), and (c) sea surface temperature (SST, °C) from moorings, color-coded to represent the 4 locations along 90 °E. Daily data are shown from May 1 to Oct 31, 2015 after 5-day smoothing. Black vertical lines denote June 1 and September 30, marking the summer monsoon period.

To highlight the role of salinity-driven stratification due to river plumes, we have started our budget analysis. Results of the 1-D calculation for the 18°N mooring in August and September are summarized in Figure 6, which shows the series of 10-day low-pass filtered observed ML temperature tendency (orange) and the temperature tendency predicted by the heat flux alone (blue). While the predicted tendency matches the observed one reasonably well in early summer, these two disagree in late summer. However, when the vertical entrainment is considered via using the PWP model, the temperature tendency (green) matches the observations (orange) better than that based on heat flux alone. In particular, the two spurious cooling events predicted by the surface heat flux are completely removed in the PWP model calculation.

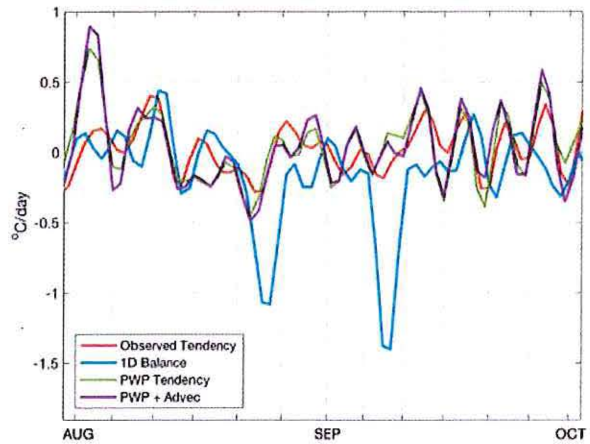

Figure 6: Time series of 10-day low-pass filtered temperature tendency (°Cday^{-1}) at 18°N for late summer (August-September) in 2015 from (orange) the observations, (blue) the 1-D heat balance, (green) the PWP model, and (purple) the PWP model plus horizontal advection. The PWP model is initialized July 31 for the simulation of late summer.

c. Effect of eddy-wind interaction on upper ocean stratification (Seo et al. 2019)

Finally, we examine the effect of surface current in the bulk formula for the wind stress, which is often referred to in the literature as the relative wind (RW) effect, in the energetics of the ocean circulation and upper ocean stratification during summer. The effect of RW on the simulated flow fields can be immediately seen from Figure 7, which compares the snapshot of the Rossby number (*Ro*). One can notice that the absolute magnitude of *Ro* in CTL is generally weaker than that of noRW. The probability density function (PDF) of *Ro*, calculated for the entire simulation period and the domain, supports this initial impression. *Ro* in excess of +0.5 is found in both model runs; however, CTL shows more regions of smaller *Ro* and fewer areas of intense *Ro*. The superposed black curve denotes the percent difference, confirming that *Ro* is reduced in CTL with the particularly strong reduction in the range of -0.8~-0.5. Therefore, the RW effect in the BoB appears to reduce preferentially the intensity of the anticyclonic eddies with relatively high *Ro*.

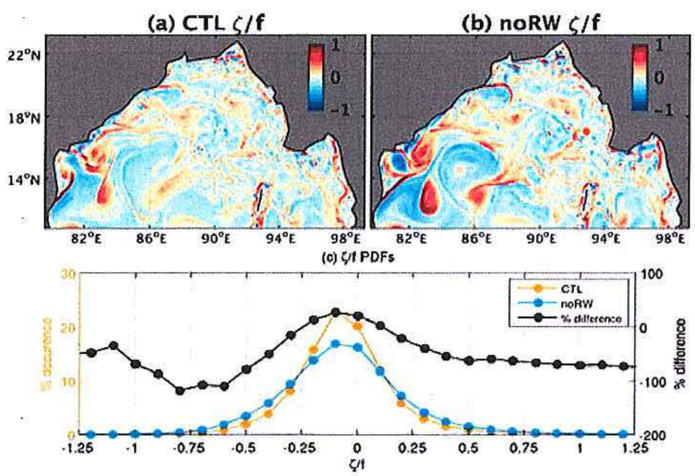

Figure 7: Snapshots of relative vorticity normalized by local Coriolis frequency (ζ/f) on June 12, 2009 from (a) CTL and (b) noRW. (c) Histograms of ζ/f over the whole domain for the summers of 2007-2015 and their percent difference.

This RW effect appears to be important for the upper ocean stratification and MLD in the BoB. Figure 8 shows the depth-longitude diagrams of the density, N^2, and S^2 over 12-15°N. The colored contours denote the lines of constant density, N^2, and S^2 for CTL and noRW, while the differences (CTL-noRW) are shown as the shading. The RW effect raises the isopycnals, resulting in higher density anomaly above the thermocline up to 25 m just below the MLD. The increase in density between the MLD and D20 is due to reduced temperature and increased salinity in CTL. As a result of increased density, N^2 is significantly enhanced in CTL below the ML and reduced near the D20. The increased N^2 in the upper isopycnals would hence explain the shallower MLD in CTL. S^2 is significantly reduced in the deeper layer, consistent with the basin-wide reduction in wind work, but near the MLD, there is a hint of increased S^2.

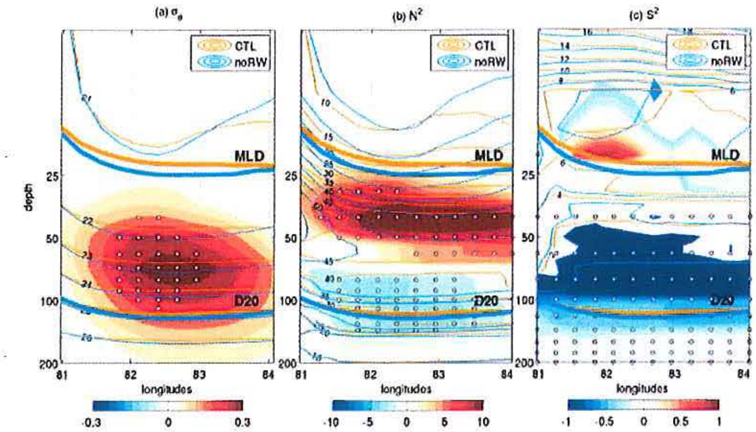

Figure 8: Depth-longitude diagrams of (a) density (σ_θ, kgm^{-3}), (b) N^2 ($10^{-5}s^{-2}$), and (c) S^2 ($10^{-5}s^{-2}$). The orange (blue) contours denote the quantities from CTL (noRW), and the color-shadings represent the difference (CTL-noRW). The thick curves at shallower (deeper) depth denote the MLD (D20). Dots denote the areas of significant difference at 95%.

It is shown that the increased N^2 is due to the dissipative effect of the RW on the vorticity dynamics through the eddy-induced Ekman vertical velocity (W). The total wind-driven vertical velocity W (W_{tot}) can be approximately decomposed into the three contributors, W due to the RW effect (W_c), W due to horizontal vorticity gradient (W_ζ), and W due to dependence of zonal wind stress to β (W_β), such that

$$W_{tot} = \underbrace{\frac{\nabla \times \tau}{\rho_0 (f+\zeta)}}_{W_c} + \underbrace{\frac{1}{\rho_0 (f+\zeta)^2}\left(\tau_x \frac{\partial \zeta}{\partial y} - \tau_y \frac{\partial \zeta}{\partial x}\right)}_{W_\zeta} + \underbrace{\frac{\beta \tau_x}{\rho_0 f^2}}_{W_\beta}$$

Here, the final term, W_β, is found to be at least an order of magnitude smaller than the first two terms, and thus it is not considered in the subsequent analysis. The percent difference between the first two terms (not shown) in CTL suggests that there is anomalous upward W_c, which is stronger by 100% than that in noRW. The actual amount of increase in the upward W_c is ~10-20 cm day^{-1}, i.e., for 120 days per each summer, this anomalous upward motion can alone raise the isopycnals by ~12-24 m. Considering other processes at work, this is broadly consistent with the D20 change.

IMPACT FOR SCIENCE

Observational analyses of intraseasonal air-sea interaction between rainfall and SST and the impacts of salinity on SST (and thus rainfall) improve our understanding of the role of oceans in MISO. Our coupled modeling study on the Arabian Sea suggests a strong downstream rainfall response arising from the coupling in the western Arabian Sea, useful important information for S2S prediction of monsoon rainfall over the Western Ghats. We have developed a spectral-based diagnostic technique, which will become available for validation of the other models for the representation of the fine-scale air-sea interaction. The impacts of fine-scale air-sea coupling on the predictability of the monsoon, MISO and MJO the Indian Ocean is not well quantified in many operational systems, so the diagnostics from this study can be applied real-time to the forecasts models. The sensitivity and predictability study based on this project will help to identify the ways to improve the representation of air-sea interaction processes under MISO in the operational models.

RELATIONSHIPS TO OTHER PROGRAMS

Through this project, I have collaborated with many PIs from ASIRI, MISO-BoB, and NASCar DRIs. The active collaboration with our partners from India and Sri Lanka will be connoting to examine and quantify the role of oceans and air-sea interactions in the monsoon precipitation and circulation.

OUTREACH

The results of the project have been introduced to visitors from India to WHOI in the past four years, including recent visitors from Ministry of Earth Sciences, Government of India. The PI is currently working with the McMullen Museum of Art at Boston College on a new exhibition entitled *Indian Ocean Current: Six Artistic Narratives.* The result from this project will be used for a theme on Changes to Monsoon and Extreme Events. The PI teaches two courses in the MIT/WHOI Joint Ph.D. Program, where the results and ideas from this project, including data analysis and modeling techniques have been incorporated. The project has provided ample opportunities for undergraduate student mentoring including S. Jongaramruang (2015), D. Smith (2016), S. Coakely (2016), C. Prend (2017), M. Shah (2018), and Y. Liu (2018).

PUBLICATIONS

Gopalakrishnan, G., A. C. Subramanian, A. J. Miller, H. Seo, and D. Sengupta, 2019: Estimation and prediction of the upper ocean circulation in the Bay of Bengal, *Deep-Sea Res. II, Revised.*

Seo, H., A. C. Subramanian, H. Song, and J. S. Chowdary, 2019: Coupled effects of ocean current on wind stress in the Bay of Bengal: Eddy energetics and upper ocean stratification. *Deep-Sea Res. II,* https://doi.org/10.1016/j.dsr2.2019.07.005.

Weller, R. A., J. T. Farrar, H. Seo, C. J. Prend, D. Sengupta, J. Sree Lekha, M. Ravichandran, and R. Venkatesen, 2019: Moored observations of the surface meteorology and air-sea fluxes in the northern Bay of Bengal in 2015. *J. Climate*, 32, 549–573.

Prend, C. J., H. Seo, R. A. Weller, J. T. Farrar, and A. Mahadevan, 2018: Impact of freshwater plumes on intraseasonal upper ocean and rainfall variability. *Deep Sea Res. II*, 161, 63–71.

Pullen, J. R. Allard, H. Seo, A. J. Miller, S. Chen, L. P. Pezzi, P. Chu, and T. Smith, 2018: Coupled ocean-atmosphere forecasting at short and medium time scales. *J. Mar. Res*, 75, 877–921.

Jin, X, Y.-O. Kwon, C. C. Ummenhofer, **H. Seo**, Y. Kosaka, and J. S. Wright, 2018: Distinct mechanisms of decadal subsurface heat content variations in the eastern and western Indian Ocean modulated by tropical Pacific SST, *J. Climate*, 31, 7751–7769

Jin, X., Y.-O. Kwon, C. C. Ummenhofer, **H. Seo,** F. U. Schwarzkopf, A. Biastoch, C. W. Böning, and J. S. Wright, 2018: Influences of Pacific Climate Variability on Decadal Subsurface Ocean Heat Content Variations in the Indian Ocean. *J. Climate*, 31, 4157–4174.

Seo, H., 2017: Distinct influence of air-sea interactions mediated by mesoscale sea surface temperature and surface current in the Arabian Sea. *J. Climate,* 30, 8061–8079.

Morrow, R., L.-L. Fu, T. Farrar, H. Seo, P.-Y. Le Traon, 2017: Ocean eddies and mesoscale variability. Satellite Altimetry Over Oceans and Land Surfaces, In D. Stammer and A. Cazenave, editors, Satellite Altimetry Over Ocean and Land Surfaces. *CRC Press, Taylor & Francis Group*

Miller, A. J., M. Collins, S. Gualdi, T. G. Jensen, V. Misra, L. P. Pezzi, D. W. Pierce, D. Putrasahan, H. Seo, and Y.-H. Tseng, 2017: Coupled Ocean-Atmosphere-Hydrology Modeling and Predictions. Chapter 20, The Science of Ocean Prediction, *J. Mar. Res.*, 75, 361–402.

Centurioni, L. R., and Co-authors, 2017: Northern Arabian Sea Circulation-Autonomous Research (NASCar): A Research Initiative Based on Autonomous Sensors. *Oceanography*, 30, 74–87

Jongaramrungruang, S., H. Seo, C. C. Ummenhofer, 2017: Intraseasonal rainfall variability in the Bay of Bengal during the Summer Monsoon: Coupling with the ocean and modulation by the Indian Ocean Dipole. *Atmos. Sci. Lett.*, 18, 88–95.

Chowdary, J. S., G. Srinivas, T. S. Fousiya, A. Parekh, C. Gnanaseelan, A. Mahadevan, H. Seo, J. A. MacKinnon, 2016: Bay of Bengal upper Ocean salinity biases and associated processes in General Circulation Models. *Oceanography,* 29, 38–49.